Three-dimensional target-oriented pre-stack migration*

C.P.A. Wapenaar** and A.J. Berkhout**

The main limitations of current 3D migration techniques do not lie in the zero-offset migration algorithm itself but in the preceding stacking process which generates the zero-offset input data. In conventional common-midpoint (CMP) stacking four problems may occur:

1. The members of a CMP gather may have different individual midpoints and, therefore, the concept of 'common midpoint' may not actually exist.
2. In situations with complex geology, reflection times in a CMP gather may not be described by a hyperbolic relationship and so the concept of 'stacking velocity' may not exist.
3. Conflicting structural dips require *different* stacking velocities.
4. One stacked event may represent information from *different* reflection points.

In the seventies and early eighties refined stacking procedures were developed, based on the dip moveout (DMO) concept (Bolondi *et al.* 1982; Hale 1984). These DMO-oriented stacking techniques (followed by post-stack migration) can be successfully applied if the aforementioned second problem does not occur. However, in 3D data sets generally all four problems occur and, as a consequence, the quality of post-stack migrated data is often far from optimum. Therefore, particularly for complicated subsurface structures, alternative techniques must be developed. The ideal procedure would be full pre-stack migration by single-shot record inversion (SSRI), followed by zero-offset (ZO) stacking (Berkhout 1984). However, for the 3D case this promising technique is still too laborious. It is obvious that, given the limitations of today's computational power, a more practical approach to 3D pre-stacking migration is required. In many practical situations seismic interpreters are mainly interested in an accurately positioned and well-resolved image of a pre-specified target zone. Hence, much work can be saved by the following two-stage procedure:

1. Apply conventional CMP processing and two-pass migration for an initial 3D evaluation of the total area under investigation.
2. Apply full 3D pre-stack migration to specific areas of interest ('target-oriented' stage).

In this paper we propose a full 3D *target-oriented* pre-stack migration scheme and discuss various theoretical and practical aspects. Also we demonstrate the validity of the target-oriented approach with the aid of a physical scale model (water tank) data example.

Principle of 3D target-oriented pre-stack migration

In this section we present the three basic steps of 3D target-oriented pre-stack migration (see also Fig. 1):

1. *Shot record redatuming*
   Target-related shot records at the acquisition surface are redatumed in a 3D sense to the upper boundary of a target zone. Each redatumed shot record simulates a single-fold multi-offset data set (including zero-offset), measured at the upper boundary of the target zone. The single-fold ZO traces are selected for further processing.
2. *ZO stacking*
   The single-fold ZO traces from all redatumed shot records are sorted per source-detector point at the upper boundary of the target zone. Next, at each point the single-fold ZO traces are summed, yielding a multi-fold ZO dataset at the upper boundary of the target zone.
3. *ZO migration*
   Full 3D ZO migration is applied to the multi-fold ZO dataset, yielding an accurately positioned and well resolved image of the target zone.

The computational diagram is shown in Fig. 2. The outlined procedure is dramatically more efficient than full 3D pre-stack migration because (i) 3D pre-stack downward extrapolation is carried out to only a limited depth (the upper boundary of the target zone) and (ii) 3D ZO migration is carried out in the target zone only. On the other hand, the outlined procedure is much more accurate than current CMP-oriented 3D procedures because 3D shot record redatuming (step 1), followed by ZO stacking (step 2), properly accounts for the distorting effects of a complex overburden and any irregular shooting geometry. Hence, *full* 3D ZO migration (step 3) is applied to *genuine* ZO data which contain

*Presented at the 48th EAEG Meeting, Ostend 1986.
**Delft University Technology, Laboratory of Seismics and Acoustics, PO Box 5046, 2600 GA Delft, The Netherlands.

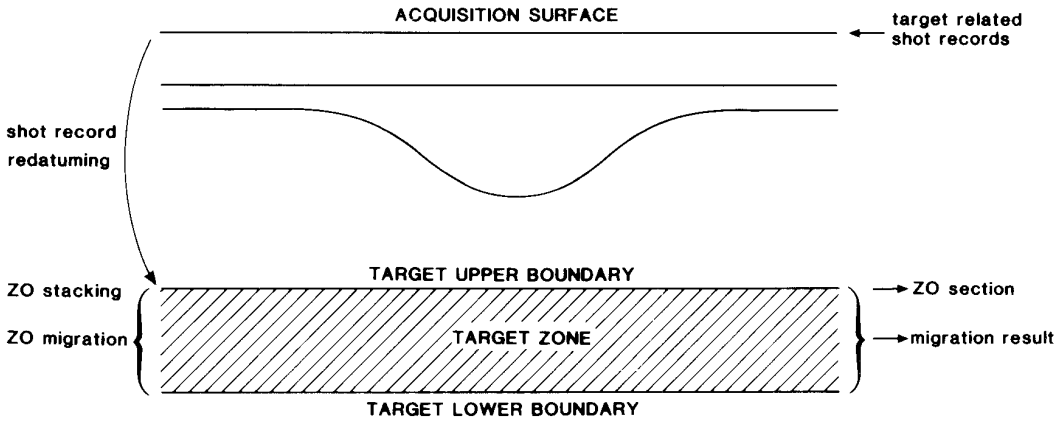

Fig. 1. There are basically three steps in target-oriented processing: (1) Pre-stack redatuming of target related shot records to the upper boundary of a target zone. (2) Stacking of the zero-offset traces for each simulated source–detector point at the upper boundary of the target zone. (3) Full 3D zero offset migration within the target zone.

undistorted wide-angle information (including properly stacked diffraction energy) from the target zone.

Note that in this target-oriented approach it is assumed that an initial 'macro subsurface model' (a description of the subsurface in terms of the main geological boundaries with average velocities and/or velocity gradients of the macro layers) is available.

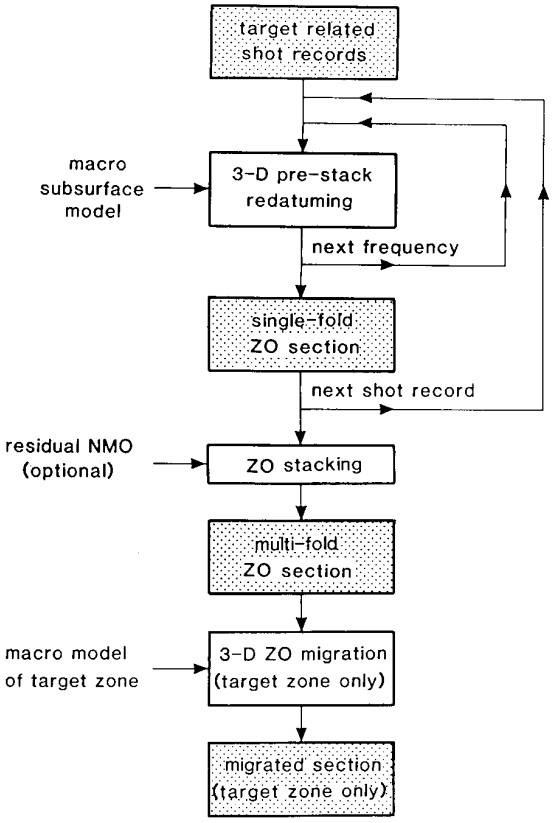

Fig. 2. Computational diagram for 3D target-oriented pre-stack migration.

Verification of the velocities in this macro subsurface model is possible by analysing the residual normal moveout (NMO) in the ZO gathers after redatuming but before stacking (if a correct macro subsurface model was used there should be no residual NMO). A further discussion on this new type of velocity analysis is beyond the scope of this paper.

We now discuss the aspects of the redatuming scheme in more detail. When designing a redatuming algorithm the following questions should be addressed.

1. Should the scheme be based on the one-way or on the two-way wave equation?
2. Should it be a full pre-stack method or should redatuming be carried out per shot record?
3. Should it be based on the acoustic approximation or is it possible to take full elastic effects into account.

The first question (one-way or two-way) can be quickly answered. One-way schemes account for primary waves only but are rather insensitive to errors in the macro subsurface model. Two-way schemes account for primary as well as multiply reflected waves, but are very sensitive to errors in the macro subsurface model. For 3D applications the robustness of the one-way approach is far more important than the multiple handling of the two-way approach. Hence, 3D pre-stack redatuming should generally be based on the one-way wave equations.

Before answering the second question (full pre-stack or shot record redatuming) we define what is meant by 'full pre-stack' redatuming. Full pre-stack redatuming involves downward extrapolation of the detectors in all common shot records, followed by re-ordering the data from common shot records into common detector records, followed by downward extrapolation of the sources in all common detector records, making use of the principle of reciprocity. Amplitudes may be correctly handled, but the data management is rather

cumbersome. When redatuming is carried out per common shot record, on the other hand, the data management is very simple because the re-ordering process is avoided (see also the next section).

Berkhout (1984) has shown that 2D shot record migration, followed by ZO stacking, is fully equivalent to 2D full pre-stack migration. From a similar analysis (not presented here) we may conclude that 3D redatuming per shot record, followed by ZO stacking, is fully equivalent to 3D full pre-stack redatuming. Hence, the amplitude handling of both methods is the same. For 3D applications it is essential that the data management is as simple as possible. Therefore 3D pre-stack redatuming should be carried out per shot record.

Last, but not least, since the earth is time-invariant, 3D pre-stack redatuming can be carried out per *monochromatic* shot record (after Fourier transforms from time to frequency). This has the important consequence that only very small portions of data need be processed at a time and that the algorithm lends itself very well for implementation on multi-CPU computers.

When addressing the third question (acoustic or full elastic redatuming) we should keep in mind that we confined ourselves already to pre-stack redatuming (per shot record) of *primary* waves. This means that both in the acoustic case and in the full elastic case the scheme should be based on inverse extrapolation of primary compressional waves.

For the acoustic case it can be shown that *true amplitude inverse* wavefield extrapolation through arbitrarily inhomogeneous media can be accomplished with the aid of generalised 'Kirchhoff summation' operators. This approach can be further generalised: the full elastic version of the generalised Kirchhoff summation operators can take into account the effect of wave conversion on the amplitudes of primary compressional waves.

Both in the acoustic and in the full elastic case our approach involves two steps: (i) computation of the Kirchhoff summation operators by forward modelling and (ii) application of the (time-reversed) operators to the pre-stack data (generalised 'spatial deconvolution', see also Fig. 3). For the 3D case we carry out these two steps independently of each other. Hence, initially all Kirchhoff summation operators are modelled (for instance by 'Gaussian beam' ray-tracing, Červený & Pšenčik 1983) and stored into a table. Next, during the actual redatuming process, the operators are read from the table and applied to the data. In this way each operator need be computed only once, while it can be used many times on the different shot records.

The question whether to use the acoustic or the full elastic approach mainly depends on the type of algorithm that is used in the initial forward modelling, and to a much smaller degree it depends on the actual redatuming algorithm itself. Hence, depending on what modelling software is available, 3D pre-stack redatuming may be based either on the acoustic or on the full elastic one-way wave equations.

We should make one more remark with respect to our table-driven redatuming approach. When the operators are modelled for a regular coarse grid of acquisition points it is necessary to interpolate the operators (not the data!) during the actual redatuming process. On the one hand this involves additional computational effort during redatuming. On the other hand, however, it may

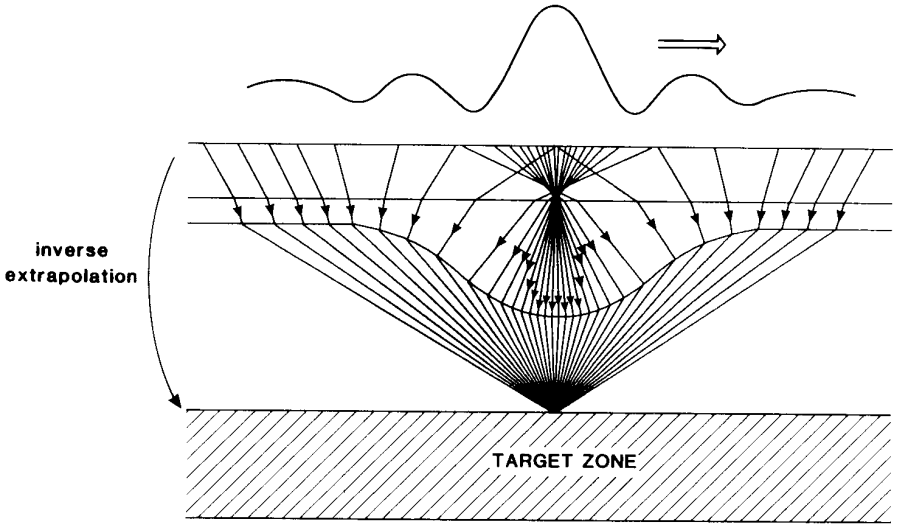

Fig. 3. Pre-stack redatuming per shot record is essentially based on inverse extrapolation of primary waves. Both the *acoustic* and the *full elastic* generalised Kirchhoff summation approach to inverse wavefield extrapolation involve the following two steps: (1) forward modelling of the operators, (2) application of the time-reversed operators to the data (generalised 'spatial deconvolution').

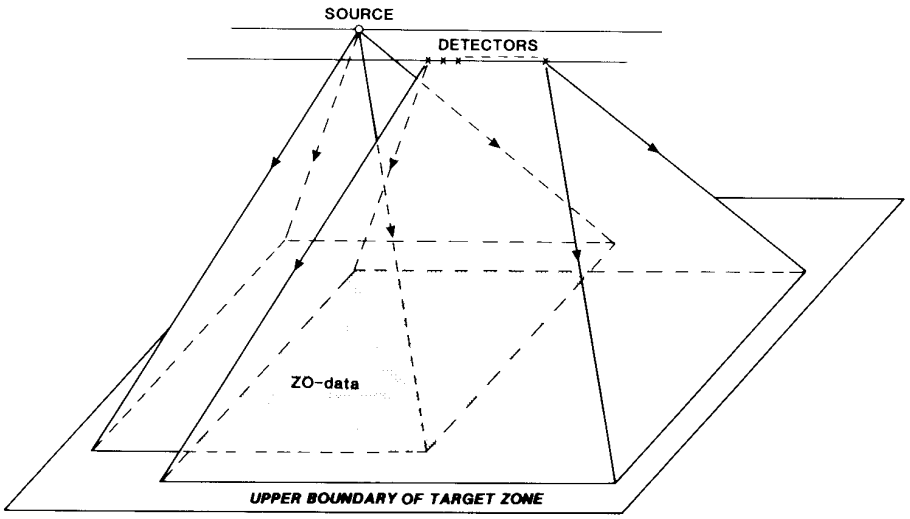

Fig. 4. Redatuming of one (monochromatic) shot record involves downward extrapolation of the source and detectors to the upper boundary of the target zone, followed by the construction of (single-fold) ZO data in the overlap area.

reduce the table size significantly and, more importantly, it enables adaptation of the operators to any irregular acquisition grid (including VSP).

Some practical aspects of 3D target-oriented pre-stack migration

In the previous section we argued that 3D pre-stack redatuming should be carried out per shot record because the data management should be as simple as possible. In this section we discuss the data management in some more detail. Therefore we consider the data flow for a pre-stack marine dataset, which typically may consist of

200 seismic lines,
200 seismic experiments (shot records) per seismic line,
100 traces (detectors) per seismic experiment,
2000 samples per trace, and
4 bytes per sample.

Hence, the total survey contains 32 Gbytes of data.

According to the computational diagram of Fig. 2, each shot record is redatumed to the upper boundary of the target zone, where for each shot record a 3D single-fold ZO section is generated. For one *monochromatic* shot record this procedure is visualised in Fig. 4. Notice that the source and detector data, which are represented at the acquisition surface by one (complex) scalar and one (complex) 1D array, respectively, are both spread out over a 2D area at the upper boundary of the target zone. Consequently, the monochromatic single-fold ZO data, which should be constructed in the overlap area, are represented by a (complex) 2D array. Hence, the amount of single-fold ZO *output* data after redatuming is much larger than the amount of single-shot record *input* data. Typically, for one broad-band single-shot input record, which contains 0.8 Mbyte of data (see above), the broad-band 3D single-fold ZO output section may consist of

200×200 traces,
500 samples per trace (target zone only), and
4 bytes per sample,

or 80 Mbytes in total, so the amount of data increases by a factor *one hundred*. Assuming that all shot records are involved in the process, the total amount of data just before ZO stacking equals one hundred times the amount of input data: 100×32 Gbytes = 3200 Gbytes!

Of course the next step in the process (ZO stacking) involves an enormous data reduction. However, the huge amount of tape I/O that would be required makes the computational diagram of Fig. 2 impracticable. If the stacking process were to be carried out inside the 'shot record loop', then the tape I/O problem would be avoided. However, for the residual NMO analysis it is essential that the stacking process is carried out outside the shot record loop.

An attractive compromise between efficiency (with respect to tape I/O) on one hand and flexibility (with respect to the stacking process) on the other hand is outlined by the modified computational diagram of Fig. 5. Notice that, according to this diagram, the processing is carried out per *cluster* of shot records. A cluster consists of, typically, one hundred shot records (for instance all shot records on one tape). *ZO stacking for all (monochromatic) shot records in one cluster* is carried out efficiently inside the shot record loop (without the possibility for residual NMO analysis). Hence, the

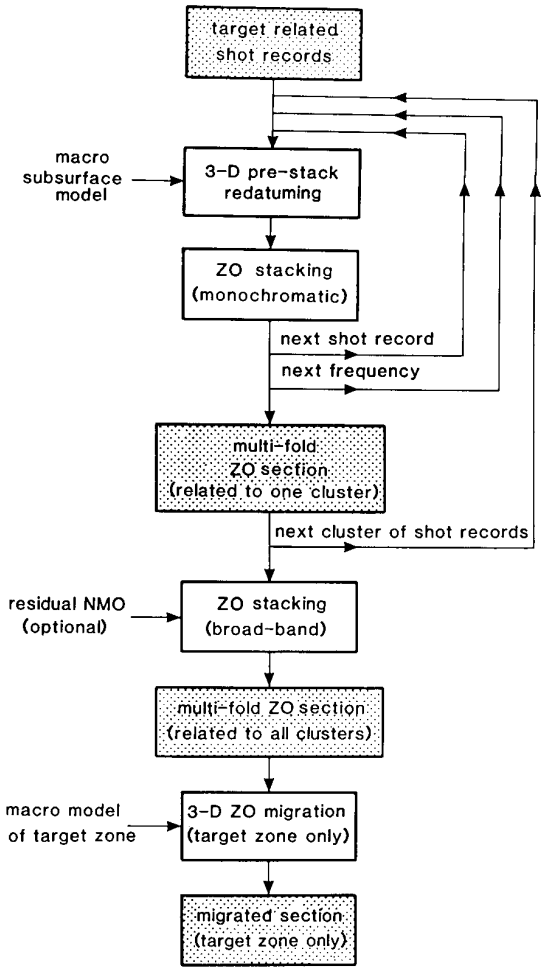

Fig. 5. Modified computational diagram for 3D target-oriented pre-stack migration. Redatuming and stacking are carried out per cluster of shot records. This allows optimum efficiency with respect to both disc I/O and tape I/O.

amount of data just before the final *ZO stacking process for all clusters* is of the same order as the amount of input data (typically 32 Gbytes). This means a significant improvement compared with the scheme discussed before (Fig. 2). Notice that the final ZO stacking process (for all clusters) takes place outside the 'cluster loop'. Hence, in this stage residual NMO analysis can be carried out for the investigation of errors in the velocities of the macro subsurface model.

Another important practical aspect, which has not been discussed so far, is the amount of required disc I/O. A cluster of shot records typically contains 80 Mbytes of data (see above). Processing of these data requires a memory overhead of typically 400 Mbytes, which is much larger than the internal computer memory. Hence, the required memory space should be reserved on *disc* and the algorithm should be designed efficiently with respect to disc I/O. Since in 3D pre-stack redatuming *no* imaging (summing over all frequencies) is performed, there is no reason to choose the 'frequency loop' as the inner loop (as in Fig. 2). Much disc I/O can be avoided if the processing of *all* shot records in a cluster is carried out per frequency component (as in Fig. 5).

For one cluster of shot records the data-flow is visualised in Fig. 6. As shown in Fig. 6a, the data are first prepared by transforming each shot record from the time domain to the frequency domain (this step is not shown in the computational diagram of Fig. 5). The actual redatuming (per frequency component) is visualised in Fig. 6b. Notice the optimum efficiency with respect to disc I/O: each frequency component is transported from disc to memory (and vice versa) only once. Finally, as is shown in Fig. 6c, the output data are transformed back from the frequency domain to the time domain (this step is also not shown in the computational diagram of Fig. 5).

Preliminary results of 3D target-oriented pre-stack migration on scale model data

In the previous sections the principle and some practical aspects of a 3D target-oriented pre-stack migration scheme were discussed. The practical implementation of the scheme can be realised nowadays on vector computers. However, at this moment much software development is still required before large real datasets can be processed. This is the subject of a project (named TRITON) being carried out at Delft University (Berkhout *et al.* 1985).

In this section we demonstrate the validity of the target-oriented migration concept and show how 3D target-oriented pre-stack migration compares with 2D target-oriented pre-stack migration (Wapenaar 1986). To do this we generated 3D multi-experiment, multi-offset data in a model tank. On the bottom of the water tank we placed the well known 'French model' (French 1975; see Fig. 7). The measurements were done just below the water surface, using two axially-symmetric piezo-electric transducers in an x_s, x_r, y positioning system (x_s = in-line coordinate of source, x_r = in-line coordinate of receiver, y = cross-line coordinate of source and receiver). By carrying out 32 experiments for a fixed source position and a variable receiver position a 32-channel common-shotpoint (CSP) gather can be simulated.

In total we modelled 64 seismic lines with 64 CSP gathers each, thus simulating a 3D marine survey with $64 \times 64 \times 32 = 131\,072$ traces. The line spacing equals 20 m (throughout this section we give the simulated dimensions, the scaling factor being 20000). The 32nd CSP gather of line 25 is shown in Fig. 8a. The smallest source–receiver offset equals 225 m and the receiver spacing equals 15 m. The time traces start at 0.84 s, the time sampling interval is 4 ms and the total trace-length

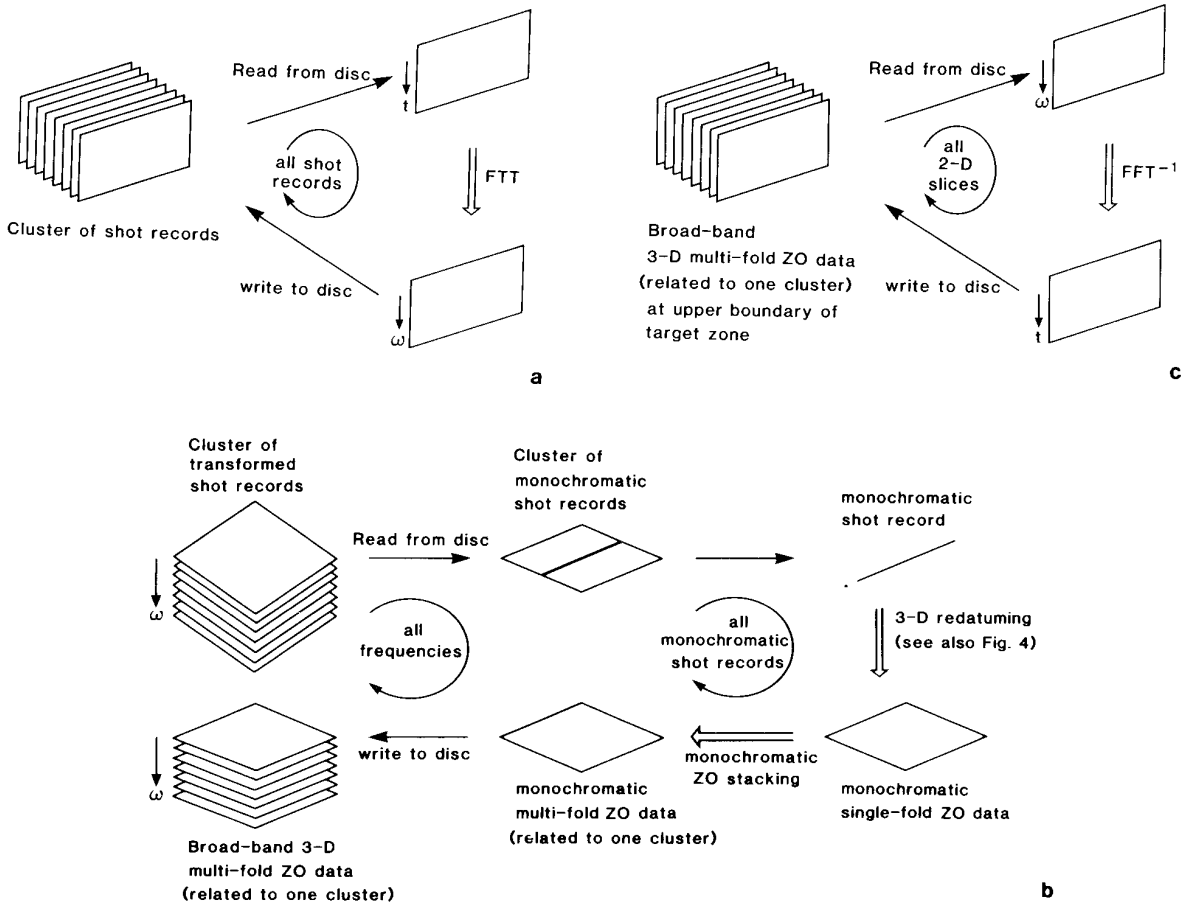

Fig. 6. The data flow for one cluster of shot records in 3D pre-stack redatuming and ZO stacking. (a) Transformation from time to frequency domain. (b) The actual redatuming and stacking. (c) Transformation from frequency to time domain.

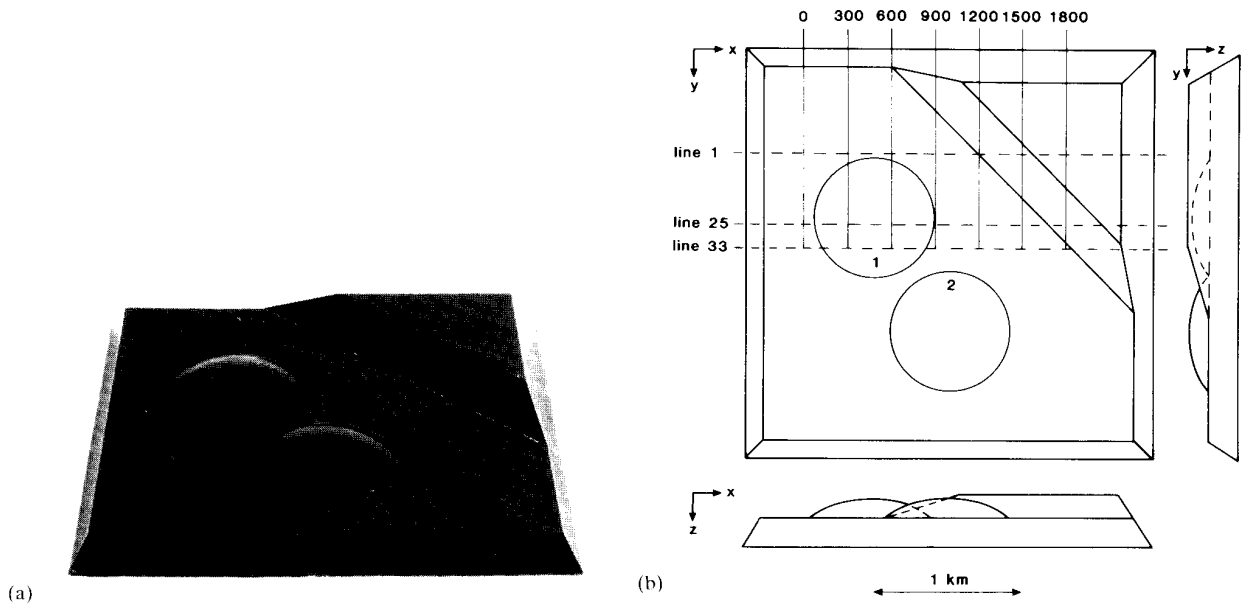

Fig. 7. The 'French model' (5 cm in the model simulate 1 km). (a) Perspective view. (b) Top-view and two side-views.

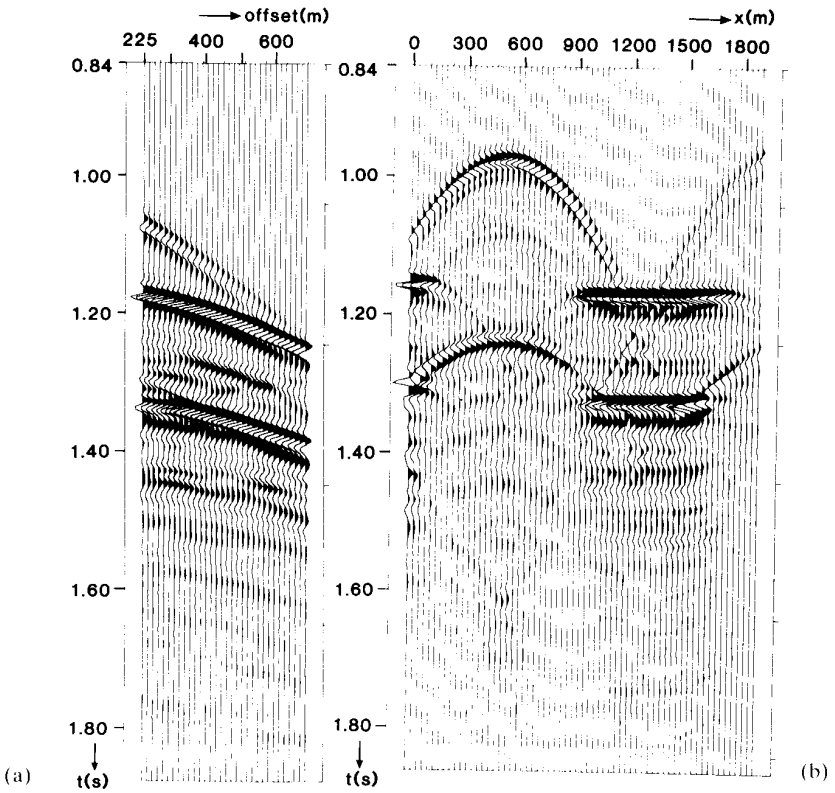

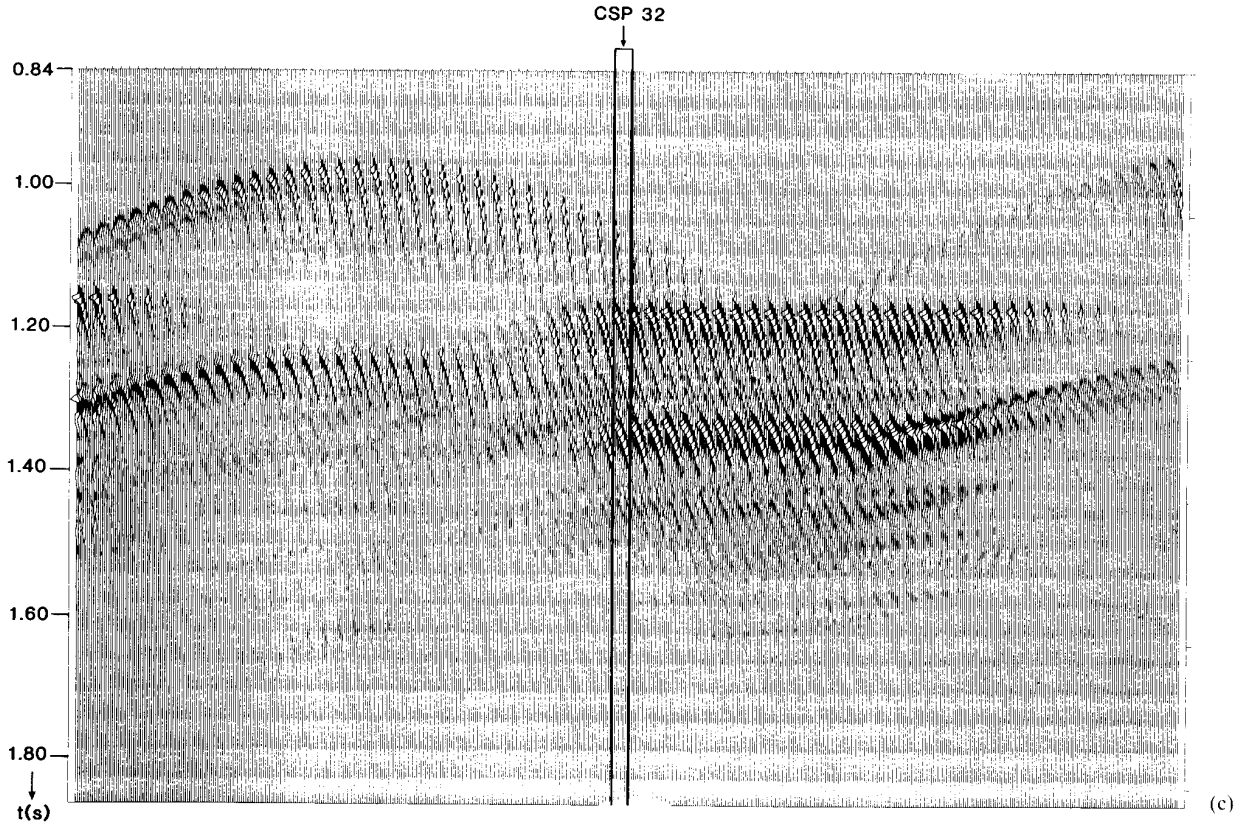

Fig. 8. 3D marine survey simulated in a model tank. (a) CSP gather (line 25, shotpoint 32). (b) CO gather (line 25, offset 225 m). (c) Seismic line 25 (64 CSP gathers).

is 256 samples. The frequency content ranges from approximately 20 to 100 Hz. A common-offset (CO) gather, selected from line 25, is shown in Fig. 8b. The offset equals 225 m and the midpoint spacing equals 30 m. Figure 8c shows all 64 CSP gathers of line 25, plotted next to each other (only every fourth trace is plotted). The shot spacing equals 30 m.

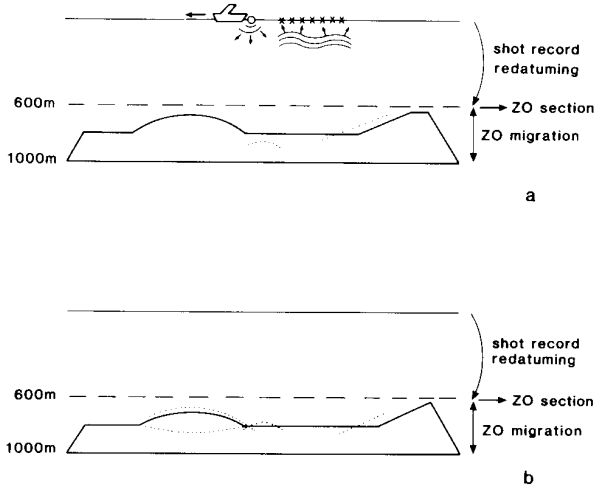

Fig. 9. Vertical 2D slices of the subsurface below lines 25 and 33, respectively. (The dotted lines indicate mispositioned events after 2D processing, see also Fig. 10.)

Vertical 2D slices of the subsurface below lines 25 and 33, respectively, are shown in Fig. 9. The upper boundary of the target zone is defined at a depth of 600 m and the lower boundary at 1000m. *Two-dimensional* redatuming of line 25 to the upper boundary of the target zone, followed by 2D ZO stacking and 2D ZO migration in the target zone yields the depth section shown in Fig. 10a. Notice that the first dome is correctly positioned (the top of this dome lies almost vertically below line 25). However, two other events are easily misinterpreted: a side-swipe reflection from the second dome is imaged just below the left end of the horizontal reflector and a side-swipe reflection from the sloping edge intersects the right end of the horizontal reflector. The same procedure applied to line 33 yields the depth section shown in Fig. 10b. Apart from aforementioned artefacts, notice also that the first dome is mispositioned and that side-swipe diffractions from the dome-edge are imaged below the dome. For clarity the erroneously positioned 'out of plane events' are indicated by dotted lines in Fig. 9. Notice that these false images are due to the 2D assumption being invalid (the 'coherent noise' just below the dome is mainly due to imperfections of the physical model, and the aliasing noise above the horizontal reflector is due to spatial under-sampling).

Three-dimensional redatuming to the upper boundary of the target zone, followed by 3D ZO stacking and 3D ZO migration in the target zone, yields a 3D depth

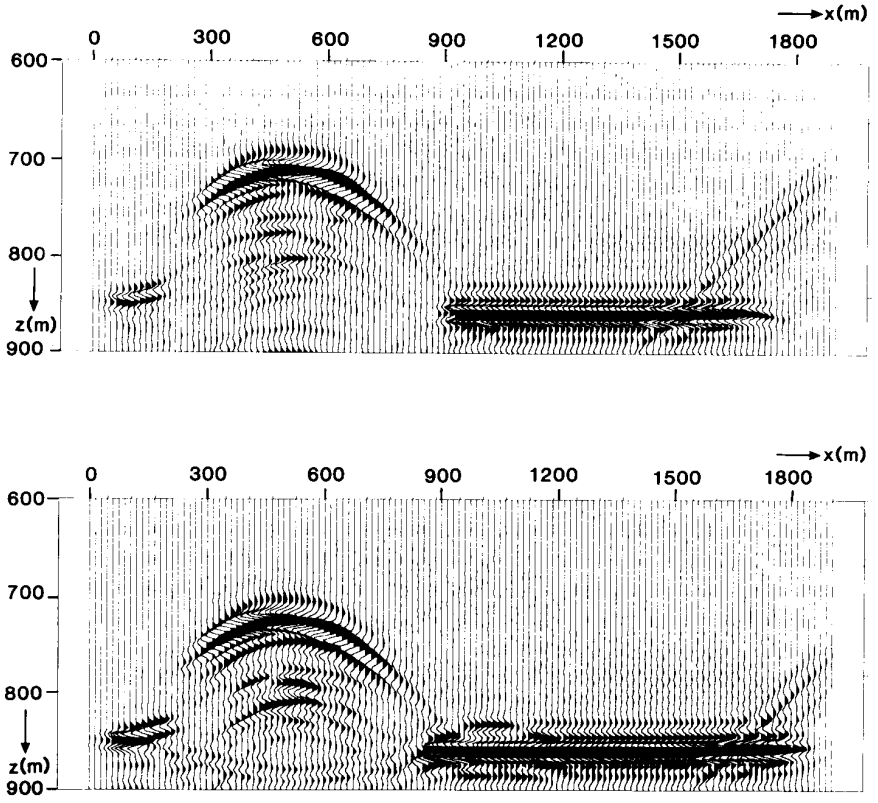

Fig. 10. Results after 2D redatuming, ZO stacking and 2D ZO migration. (a) Line 25. (b) Line 33.

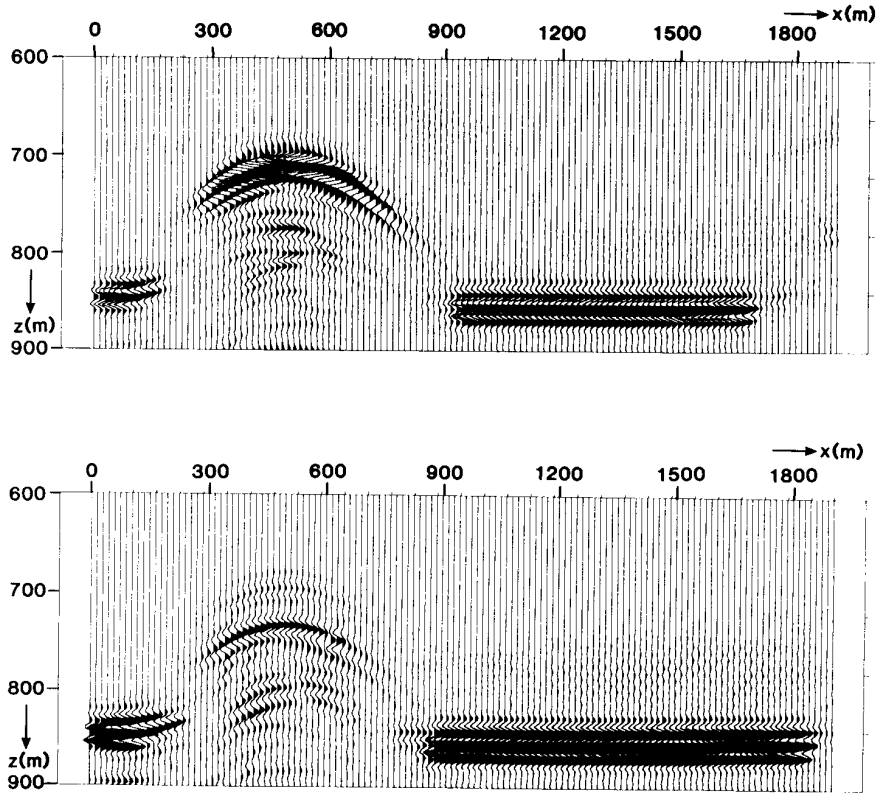

Fig. 11. Results after 3D redatuming, ZO stacking and 3D ZO migration. (a) Line 25. (b) Line 33.

section. 2D slices of this section vertically below lines 25 and 33 are shown in Fig. 11a and b, respectively. To avoid spatial aliasing related to the line spacing, we used an operator angle of 15° in the cross-line direction. Therefore a high spatial *resolution* may not be expected in the cross-line direction. However, the *positioning* of most events is now correct, in spite of the small operator angle: all the above-mentioned side-swipe reflections and diffractions disappeared, which has for example improved the lateral continuity below the horizontal reflector.

The limited cross-line operator angle accounts for the fact that the algorithm did not produce a new image of the sloping edge at the correct position. Therefore we carried out another experiment, using a finer line spacing (10 m instead of 20 m) and a wider cross-line operator angle (30° instead of 15°). Also we reduced the detector interval (12 m instead of 15 m) to suppress the aliasing noise above the horizontal reflector. A vertical 2D slice of the subsurface below line 1 is shown in Fig. 12a. The result after 2D redatuming, ZO stacking and ZO migration of line 1 is shown in Fig. 12b. Note the strong side-swipe reflection of dome 1 and the mispositioned sloping edge. A 2D slice below line 1 of the result after 3D redatuming, ZO stacking and ZO migration is shown in Fig. 12c. Note that the side-swipe reflection of dome 1 disappeared for the greater part and that the sloping edge is positioned correctly. Finally, in Fig. 12d we show a 2D slice of the *unmigrated* 3D ZO section (after 3D redatuming and ZO stacking) at the upper boundary of the target zone. Notice that these ZO data in the *time domain* can be easily interpreted because they are constructed at a level just above the zone of interest (the propagation distortions of the overburden have been eliminated). In fact these unmigrated data are very close to the migrated data in Fig. 12c. Hence, 3D shot record redatuming followed by ZO stacking at the upper boundary of the target zone represents a more costly but superior alternative to conventional CMP stacking at the acquisition surface.

Conclusions

CMP methods require (i) a regular shooting geometry such that the concept of a common midpoint exists and (ii) limited structural complexity such that the concept of stacking velocity exists. If one of the conditions is not fulfilled, as is often the case in 3D seismics, then the CMP method should be abandoned.

Shot record redatuming to a target zone, followed by ZO stacking (and ZO migration in the target zone), is far

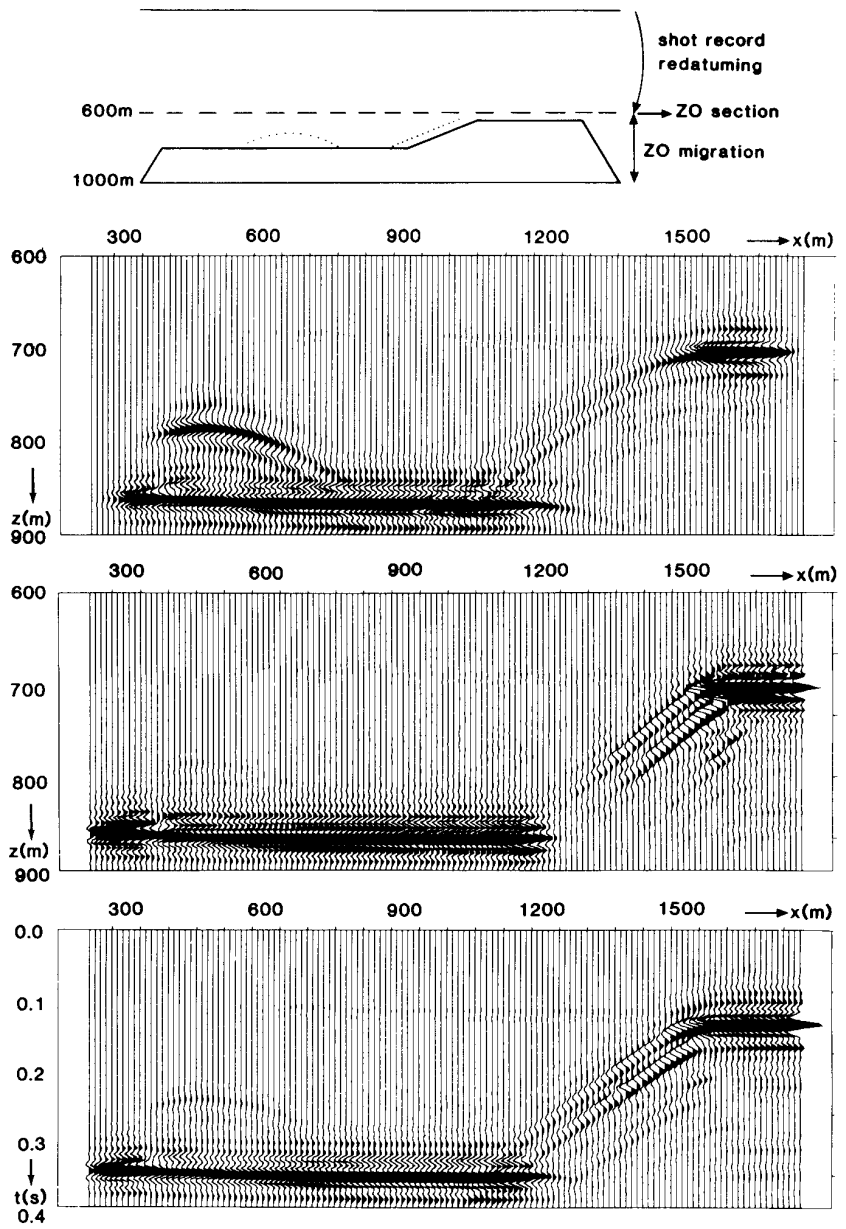

Fig. 12. Results of a new experiment, using a finer line spacing. (a) A vertical 2D slice of the subsurface below line 1 (the dotted lines indicate mispositioned events after 2D processing). (b) Result after 2D redatuming, ZO stacking and 2D ZO migration (line 1). (c) Result after 3D redatuming, ZO stacking and 3D ZO migration (line 1). (d) *Unmigrated* ZO data after 3D redatuming and ZO stacking (line 1).

superior to the CMP method for the following reasons:

1. *no* regular shooting geometry is required because redatuming is carried out per single-shot record;
2. structurally complex geologies are allowed because shot records obey the wave equation (so redatuming may be carried out to any desired degree of accuracy).

Furthermore, this *target-oriented* approach appears to be an economically very interesting solution for the 3D situation, because full 3D migration is carried out only in the zone where an accurately positioned and well-resolved image is required.

It may be expected that the combination of 3D shot record redatuming and ZO stacking will play a key role in future seismic processing.

Acknowledgments

The investigations were supported by the Netherlands Foundation for Earth Science Research (AWON) with financial aid from the Netherlands Technology Foundation (STW). Computational support was obtained from Cray Research, Inc.

Received 30 April 1986; accepted 3 February 1987.

References

BERKHOUT, A.J. 1984. Seismic migration: Imaging of acoustic energy by wave field extrapolation: B Practical aspects. Elsevier Science Publishing Company.

BERKHOUT, A.J., WAPENAAR, C.P.A., BLACQUIÈRE, G. & KINNEGING, N.A. 1985. Triton: A three-year research proposal on three-dimensional target-oriented migration, Delft University of Technology.

BOLONDI, G., LOINGER, E. & ROCCA, F. 1982. Offset continuation of seismic sections. Geophysical Prospecting 30, 813–828.

ČERVENÝ, V. & PŠENČIK, I. 1983. Gaussian beams and paraxial ray approximation in three-dimensional elastic inhomogeneous media. Journal of Geophysics 53, 1–15.

FRENCH, W.S. 1975. Computer migration of oblique seismic reflection profiles. Geophysics 40, 961–980.

HALE, D. 1984. Dip-moveout by Fourier transform. Geophysics 49, 741–757.

WAPENAAR, C.P.A. 1986. Pre-stack migration in two and three dimensions. PhD thesis, Delft University of Technology.